# cmgh

ORIGINAL RESEARCH

Optogenetic Activation of Cholinergic Enteric Neurons Reduces Inflammation in Experimental Colitis

Ahmed A. Rahman,[1] Rhian Stavely,[1] Weikang Pan,[1] Leah Ott,[1] Kensuke Ohishi,[1,2] Takahiro Ohkura,[1] Christopher Han,[1] Ryo Hotta,[1] and Allan M. Goldstein[1]

[1]Department of Pediatric Surgery, Massachusetts General Hospital, Harvard Medical School, Boston, Massachusetts; and
[2]Drug Discovery Laboratory, Wakunaga Pharmaceuticals Company, Ltd, Akitakata, Hiroshima, Japan
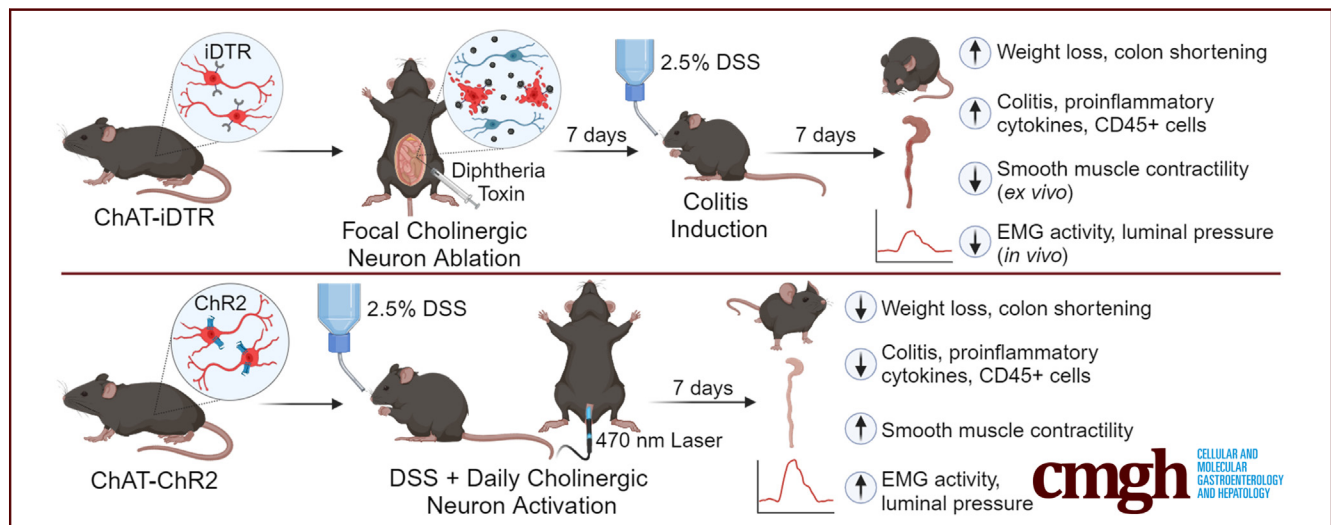
SUMMARY

The enteric nervous system, residing within the intestinal wall, regulates many important physiological functions of the gastrointestinal tract via its intrinsic microcircuitry, including motility, absorption, secretion, and intestinal immunity. Intestinal inflammation impacts enteric neuronal structure and function, and cholinergic signaling has an important role in modulating inflammation. Optogenetic activation of enteric cholinergic neurons can reduce inflammatory indices of colitis and can be explored as a potential treatment for inflammatory bowel disease.

BACKGROUND & AIMS: Intestinal inflammation is associated with loss of enteric cholinergic neurons. Given the systemic anti-inflammatory role of cholinergic innervation, we hypothesized that enteric cholinergic neurons similarly possess anti-inflammatory properties and may represent a novel target to treat inflammatory bowel disease.

METHODS: Mice were fed 2.5% dextran sodium sulfate (DSS) for 7 days to induce colitis. Cholinergic enteric neurons, which express choline acetyltransferase (ChAT), were focally ablated in the midcolon of *ChAT::Cre;R26-iDTR* mice by local injection of diphtheria toxin before colitis induction. Activation of enteric cholinergic neurons was achieved using *ChAT::Cre;R26-ChR2*

mice, in which ChAT+ neurons express channelrhodopsin-2, with daily blue light stimulation delivered via an intracolonic probe during the 7 days of DSS treatment. Colitis severity, ENS structure, and smooth muscle contractility were assessed by histology, immunohistochemistry, quantitative polymerase chain reaction, organ bath, and electromyography. In vitro studies assessed the anti-inflammatory role of enteric cholinergic neurons on cultured muscularis macrophages.

RESULTS: Ablation of ChAT+ neurons in DSS-treated mice exacerbated colitis, as measured by weight loss, colon shortening, histologic inflammation, and CD45+ cell infiltration, and led to colonic dysmotility. Conversely, optogenetic activation of enteric cholinergic neurons improved colitis, preserved smooth muscle contractility, protected against loss of cholinergic neurons, and reduced proinflammatory cytokine production. Both acetylcholine and optogenetic cholinergic neuron activation in vitro reduced proinflammatory cytokine expression in lipopolysaccharide-stimulated muscularis macrophages.

CONCLUSIONS: These findings show that enteric cholinergic neurons have an anti-inflammatory role in the colon and should be explored as a potential inflammatory bowel disease treatment. *(Cell Mol Gastroenterol Hepatol 2024;17:907–921; https://doi.org/10.1016/j.jcmgh.2024.01.012)*

Keywords: Enteric Nervous System; Cholinergic Neurons; Inflammatory Bowel Disease; Colitis; Optogenetics.

Inflammatory bowel disease (IBD), including ulcerative colitis and Crohn's disease, is a chronic inflammatory disorder of the gastrointestinal (GI) tract characterized by immune-mediated disruption of intestinal homeostasis.[1] It affects 3 million people in the United States,[2,3] with an increasing incidence among children worldwide.[4] Current therapies for IBD have serious adverse effects and often lose efficacy over time. Among patients with Crohn's disease, 70%–90% will require surgical resection of the affected intestine during their lifetime, with 40% of these patients undergoing multiple surgeries.[5] Moreover, IBD is associated with the development of severe complications, including fibrosis and strictures, enteric fistulas, perianal disease, colon cancer, impaired psychosocial functioning, and reduced quality of life. A significant unmet need exists for newer therapies that are safe, effective, durable, and well tolerated.

The enteric nervous system (ENS) is a complex neuronal network that resides within the intestinal wall and regulates many important physiological functions of the GI tract via its intrinsic microcircuitry,[6] including motility, absorption, secretion, and intestinal immunity. Although the ENS regulates immunity, intestinal inflammation in turn impacts enteric neuronal structure and function,[7] with consequences to the GI tract that include adverse effects on motility. Cholinergic signaling is known to have an important role in modulating inflammation. The cholinergic anti-inflammatory pathway (CAIP), for example, refers to a signaling pathway in which the vagus nerve suppresses inflammatory cytokine release. Conversely, intestinal inflammation is associated with reduced vagus nerve activity and imbalances in sympathetic and parasympathetic tone.[8,9] Electrical stimulation of vagal efferents, which primarily release acetylcholine (ACh), signals to activated macrophages via the α7-nicotinic ACh receptor (α7nAChR), leading to inhibition of the release of proinflammatory cytokines.[10–13] Although early studies of CAIP as a treatment of IBD are encouraging,[14–16] how vagus nerve stimulation affects inflammation in the setting of IBD remains unclear. First, the distal colon is sparsely innervated by the vagus nerve.[17] Second, vagal efferents do not interact directly with macrophages in the gut, but rather indirectly via cholinergic myenteric neurons whose nerve endings are in close proximity to resident muscularis macrophages.[18] These observations led us to the novel hypothesis that intrinsic cholinergic neurons possess anti-inflammatory properties in the gut and therefore can be leveraged for the treatment of IBD.

In experimental models of colitis, proinflammatory mediators suppress neurotransmission by cholinergic neurons,[19] which comprise roughly 70% of all enteric neurons. Dysregulation in enteric cholinergic signaling is a prominent feature of models of acute and chronic intestinal inflammation.[20,21] Furthermore, local ACh administration via enema attenuates inflammation in dextran sulfate sodium (DSS) induced acute colitis.[22] These findings support a role for intrinsic cholinergic neurons in intestinal inflammation, but the mechanism is unknown. We hypothesize that inflammation-mediated ENS injury impairs its immunoregulatory function, thereby exacerbating the underlying intestinal inflammation. We therefore propose that selective activation of cholinergic enteric neurons will reduce the severity of colitis. In this study, we tested the effect of ablating cholinergic enteric neurons on inflammation and dysmotility in DSS-induced colitis. Furthermore, we investigated whether selective activation of enteric cholinergic signaling is able to attenuate DSS-induced colitis. Our findings support an important role for enteric cholinergic innervation in colitis and illuminate its potential as a novel therapeutic strategy for the treatment of IBD.

Results

Ablation of Cholinergic Enteric Neurons Exacerbates the Severity of DSS-Induced Colitis

To determine the role of enteric cholinergic neurons in colonic inflammation, we selectively ablated choline acetyltransferase (ChAT) neurons by focal injection of diphtheria toxin (DT) into the colonic wall of ChAT-inducible diphtheria toxin receptor (iDTR) mice, followed by induction of acute colitis starting 7 days after DT injection using 2.5% DSS in the drinking water for 7 days (Figure 1A, ablated). Seven days after DT injection, successful ablation of ChAT neurons was confirmed by immunostaining for vesicular acetylcholine transporter (VAChT) and the pan-neuronal marker Hu (Figure 1B and C). To assess whether DT injection causes off-target effects, we performed immunostaining of the injection site with antibodies to the pan-neuronal marker Hu and to neuronal nitric oxide synthase (nNOS). Results were compared between the injection site (Figure 2A, top row) and an adjacent region away from the injection (Figure 2A, bottom row). Although VAChT expression is absent 7 days after DT injection, nNOS+ neurons are unaffected (Figure 2A). We also assessed CD45 immunoreactivity to determine whether DT-mediated

ablation leads to an inflammatory response and found no increase in the number of CD45+ cells (Figure 2*B*).

DSS treatment was associated with weight loss (day 7, as a percentage change of body weight relative to day 0: 81.6% $\pm$ 1.8% vs 103.0% $\pm$ 1.6%; $P < .001$), splenomegaly (103.5 $\pm$ 4.4 vs 63.6 $\pm$ 2.5 mg; $P < .001$), and colonic shortening (54.7 $\pm$ 1.6 vs 81.5 $\pm$ 3.5 mm; $P < .001$) compared with naïve mice that did not receive DSS or undergo neuronal
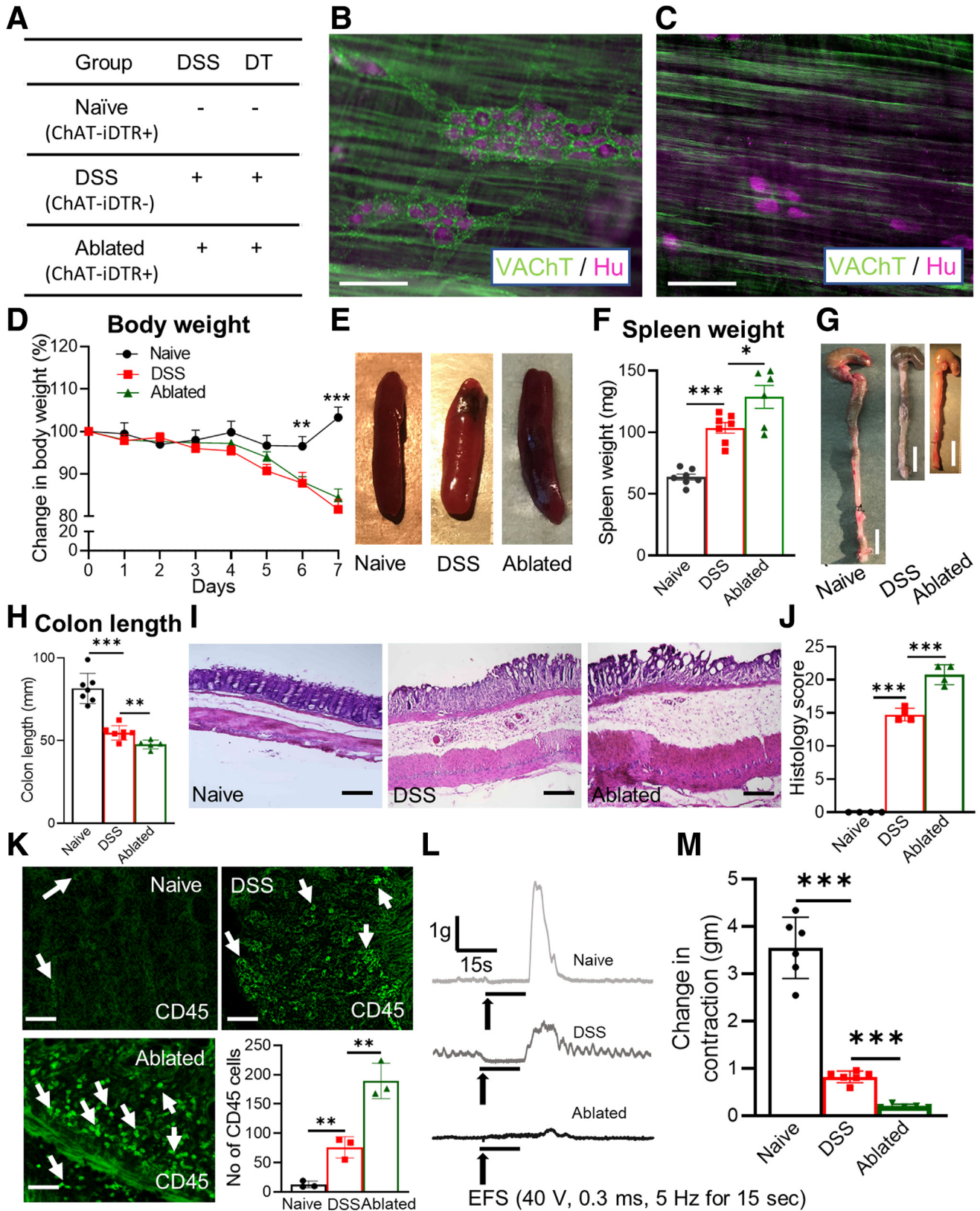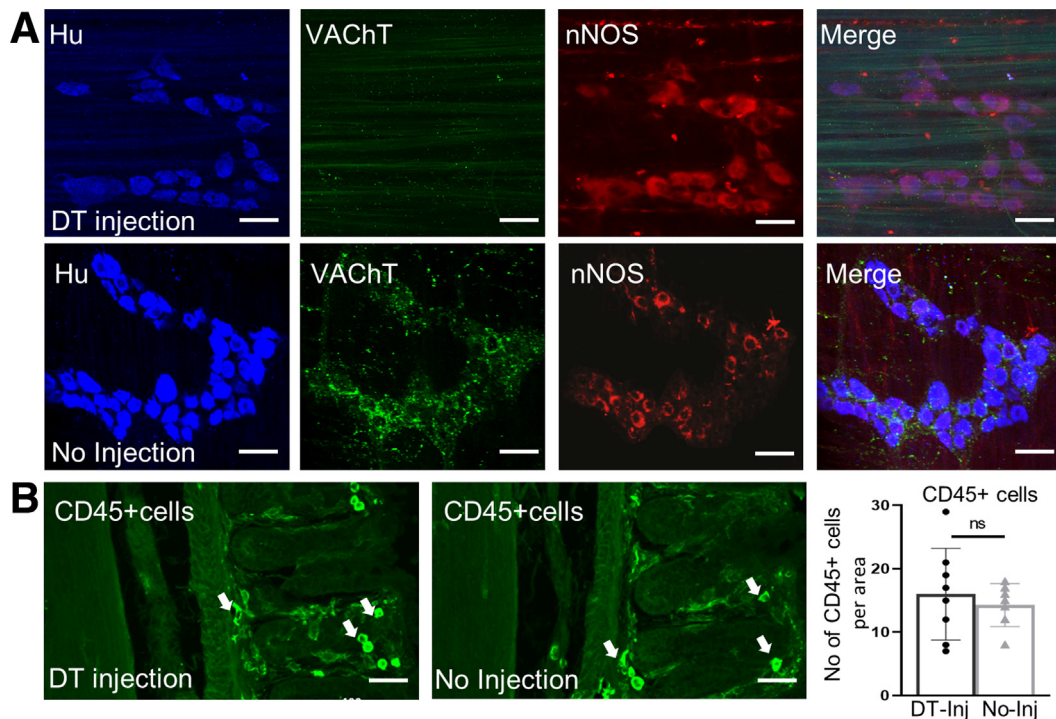
Figure 2. DT injection specifically ablates cholinergic enteric neurons. (*A*) Off-target effects of DT injection on noncholinergic neurons were assessed by immunostaining for pan-neuronal marker, Hu, and nNOS at the site of DT injection (*top row*) and at a site away from the injection (*bottom row*) in the colons of ChAT-iDTR+ mice. DT caused selective ablation of VAChT+ neurons, with no obvious effect on nNOS+ neurons as compared with panel A. (*B*) DT injection also did not cause an immune response, as noted by the absence of an increase in CD45+ cells at the injection site. *Scale bars*: 100 μm. Inj, injection.

ablation (Figure 1*A* and *D–H*). As expected, DSS led to histologic evidence of inflammation and CD45$^+$ cell infiltration (Figure 1*I–K*). Colon muscle contractility was measured by electrical field stimulation (EFS) using a standard organ bath technique. In untreated colon, EFS induced a typical biphasic response characterized by relaxation/quiescence followed by a rebound contraction at the end of stimulation.[23] The EFS-induced contraction was reduced significantly in DSS-treated mice (0.8 $\pm$ 0.1 vs 3.5 $\pm$ 0.3 g; $P < .001$) compared with naïve mice that did not receive DSS (Figure 1*L* and *M*).

Selective ablation of cholinergic neurons significantly exacerbated the severity of DSS-induced colitis. Although weight loss in these mice was similar to nonablated DSS mice (Cre-negative mice treated with both DSS and DT injection), splenomegaly and colonic shortening were increased (Figure 1*D–H*). The histologic score showed significantly worse inflammation (20.7 $\pm$ 0.7; $P < .001$), as was the extent

of CD45$^+$ cell infiltration (189 $\pm$ 17.5; $P < .01$) (Figure 1*I–K*). In addition, EFS-induced smooth muscle contraction was abolished almost completely (0.2 $\pm$ 0.02 g; $P < .001$) in DSS-treated, ChAT-ablated mice (Figure 1*L* and *M*).

Optogenetic Activation of Cholinergic Enteric Neurons Reduces the Severity of DSS-Induced Colitis

To characterize the effect of enteric cholinergic innervation in colitis, we generated ChAT–channelrhodopsin-2 (ChR2) mice in which cholinergic neurons express the light-gated channelrhodopsin and tdtomato (tdT). Based on immunohistochemistry for VAChT, 80% of cholinergic enteric neurons expressed tdT (Figure 3*A*). We used optogenetics to specifically activate these ChAT-ChR2–expressing neurons. Blue light stimulation (BLS) induced smooth muscle contraction (3.8 $\pm$ 0.3 g) that was equivalent to the

Figure 1. (*See previous page*). Ablation of cholinergic neurons exacerbates DSS-induced colitis. (*A*) Experimental and control groups are shown. DT-mediated ablation of myenteric cholinergic neurons in the colon of ChAT-iDTR+ mice was confirmed by comparing immunostaining for anti-VAChT and pan-neuronal marker Hu (*B*) before and (*C*) after DT injection. Mice receiving DSS showed (*D*) weight loss (naïve and DSS, n = 7; ablated, n = 5), (*E* and *F*) splenomegaly (naïve and DSS, n = 7; ablated, n = 6), and (*G* and *H*) colonic shortening (naïve and DSS, n = 7; ablated, n = 5), as compared with naïve mice, with the greatest difference in those receiving DT injection. (*I* and *J*) Histologic score (naïve, n = 4; DSS, n = 4; ablated, n = 4) and (*K*) CD45$^+$ cell counts (n = 3 per group) were increased significantly after ablation of cholinergic neurons in DSS-induced colitis. (*L*) Representative traces of mechanical response to electrical field stimulation (EFS) are shown. (*L* and *M*) EFS does not induce smooth muscle contraction in ChAT-ablated mice (naïve and DSS, n = 6; ablated, n = 5). *Scale bars*: 50 μm (*B, C, I,* and *K*); 10 mm (*G*). Data shown are means $\pm$ SEM. *$P < .05$, **$P < .01$, and ***$P < .001$.
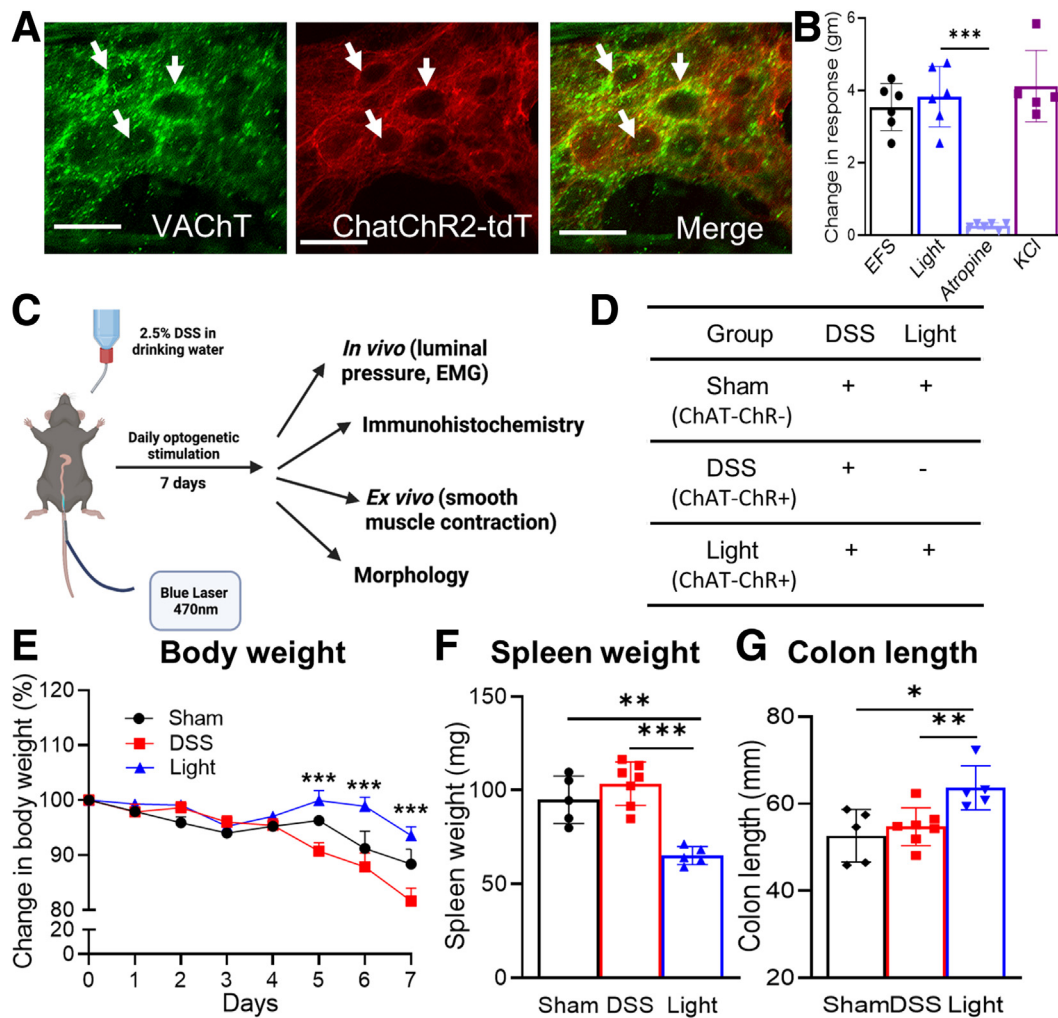
Figure 3. **Optogenetic activation of enteric cholinergic signaling reduces inflammatory indices in DSS-induced colitis.** (*A*) ChAT-ChR2 mice co-express tdT and VAChT, confirming cholinergic-specific expression of ChR2 in myenteric neurons (*white arrows*). (*B*) BLS leads to smooth muscle contractility in colons isolated from ChAT-ChR2 mice, similar to the response seen with EFS and KCl, and this response is abrogated by pretreatment with atropine (n = 6). (*C*) Mice were treated with DSS for 7 days, during which they received daily intraluminal BLS to activate colonic cholinergic neurons. (*D*) Control groups included sham and DSS groups, as shown. Weight loss was reduced markedly in the (*E*) Light group (sham, n = 5; DSS, n = 7; light, n = 5), as was (*F*) splenomegaly (sham, n = 5; DSS, n = 7; light, n = 5). (*G*) Colonic shortening (sham, n = 5; DSS, n = 7; light, n = 5) also was preserved. *Scale bars*: 50 μm. Data are shown as means ± SEM. *$P < .05$, **$P < .01$, and ***$P < .001$.

contraction elicited by EFS (3.5 ± 0.3 g) or KCl administration in the organ bath (4.1 ± 0.4 g) (Figure 3*B*). This response was abrogated by the addition of atropine (0.3 ± 0.03 g; $P < .001$), confirming that it resulted from cholinergic signaling (Figure 3*B*).

To determine how cholinergic neurons in the colon impact the severity of DSS-induced colitis, BLS was performed daily during the 7-day DSS treatment using an intraluminal optogenetic probe inserted through the rectum. This probe shines a light for a length of 3 cm in the distal colon. BLS was applied as 10-ms pulses at 10 Hz for 10 seconds, followed by a 20-second break, for a total of 30 minutes each day (Figure 3*C*). This group was designated as the *light group*. Control groups consisted of sham mice, which received both DSS and BLS but did not express ChR2; and DSS mice, which express ChAT-ChR2 and receive DSS,

but no BLS (Figure 3*D*). Local activation of the cholinergic system by BLS reduced the clinical indices of colitis, as indicated by less weight loss (day 7 relative to day 0: 93.5% ± 1.6% vs 81.6% ± 2.4%; $P < .001$), reduced spleen weight (65.1 ± 2.1 vs 103.5 ± 4.4 mg; $P < .001$), and increased colon length (63.7 ± 2.3 vs 54.7 ± 1.6 mm; $P < .01$) compared with DSS treatment alone (Figure 3*E–G*).

Optogenetic activation of cholinergic neurons also mitigated DSS-induced injury to the colon, attenuating the histologic colitis score (11.3 ± 0.8 vs 14.8 ± 0.5; $P < .01$) and CD45$^+$ cell infiltration (39.0 ± 7.0 vs 76.0 ± 10.6; $P < .05$) compared with DSS treatment alone (Figure 4*A–D*). Furthermore, fecal lipocalin (Lcn)-2 ($P < .01$) (Figure 4*F*) and messenger RNA (mRNA) expression of the intestinal proinflammatory cytokines *Il1b* (0.1 ± 0.1 2 vs 4.0 ± 0.3 $2^{-\Delta Ct}$ (delta CT method for calculating relative gene expression) $P < .001$),
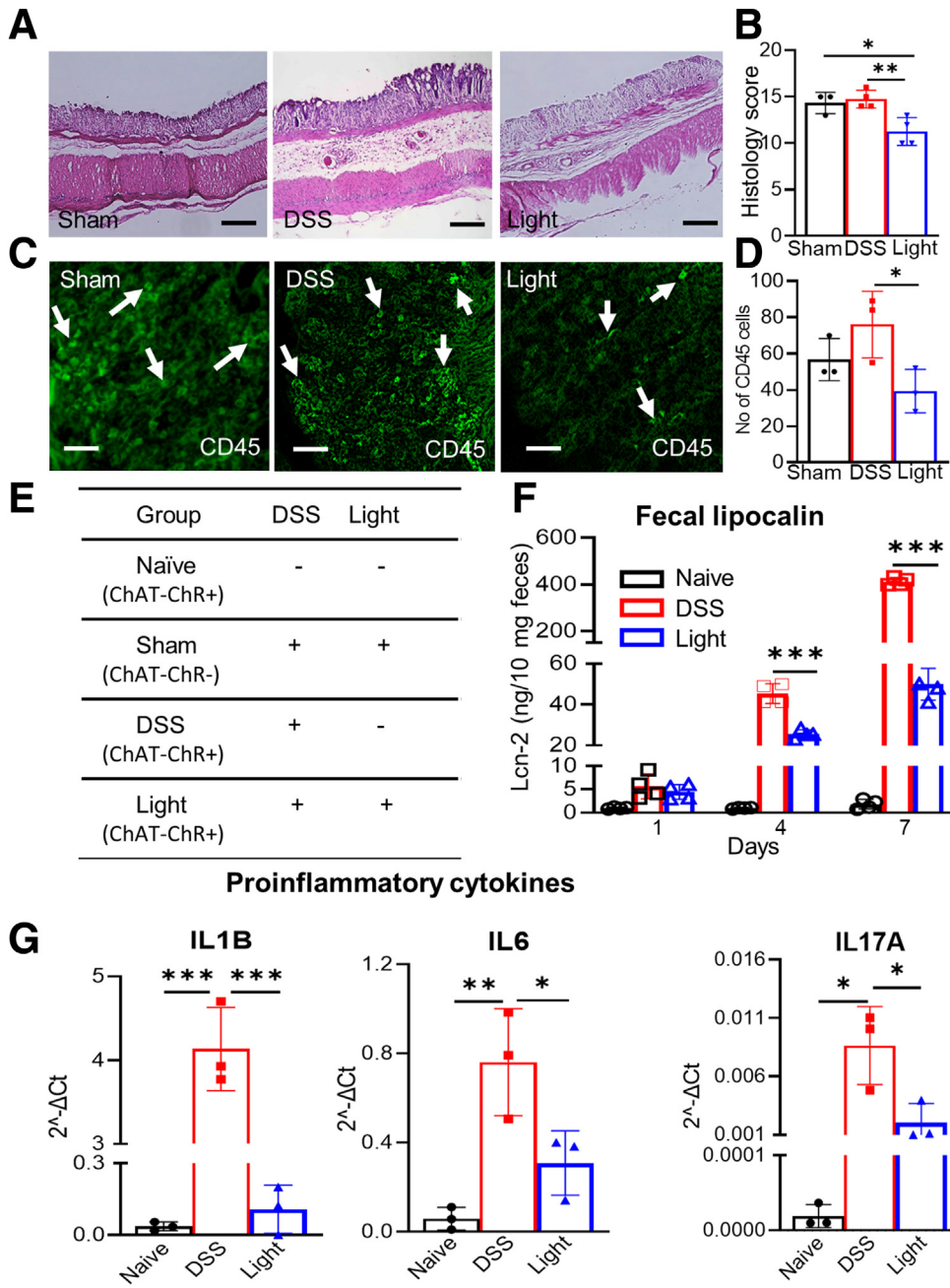
Figure 4. Selective activation of cholinergic neurons by BLS reduces inflammatory markers in DSS colitis. Optogenetic stimulation in DSS-induced colitis reduced inflammation based on (*A* and *B*) histology (sham, n = 3; DSS and light, n = 4) and (*C* and *D*) CD45$^+$ cell infiltration (n = 3) compared with both (*E*) sham and DSS groups. (*F*) Fecal lipocalin-2 levels were low in naïve mice, increased with DSS treatment, and the DSS-induced increase in fecal lipocalin was blunted on days 4 and 7 in mice receiving concurrent BLS (n = 4). Optogenetic activation of cholinergic neurons also lowered mRNA expression of multiple proinflammatory cytokines. *Scale bars*: 50 μm. Data are shown as means ± SEM. n = 3 mice per group. *P < .05, **P < .01, and ***P < .001.

Il6 (0.3 ± 0.1 2 vs 0.8 ± 0.1 2$^{-\Delta Ct}$; *P* < .05), and *Il17a* (0.002 ± 0.001 2 vs 0.009 ± 0.002 2$^{-\Delta Ct}$; *P* < .05) all were down-regulated markedly by BLS during DSS treatment (Figure 4*G*).

It is known that several hematopoietic cell types aside from cholinergic neurons, including T cells, B cells, and innate lymphoid cells, express ChAT. We therefore performed flow cytometry on the colons of ChAT-ChR2 mice, in which all ChAT+ cells are labeled with tdT, using an antibody to CD45 to analyze the relative proportion of ChAT-expressing cells. As shown in Figure 5*A*, flow cytometry shows that 2.9% of all cells in the DSS-treated colon are ChAT+. Of these, 86% are CD45-negative, whereas only 14% are CD45+, hematopoietic cells. Because the CD45-negative population can include both cholinergic neurons and tuft cells, which are known producers of ACh, we performed immunofluorescence using the tuft cell–specific marker, doublecortin-like kinase protein 1 (Dclk1). Interestingly, we found that colonic tuft cells do not express ChAT (Figure 5*B*), meaning that these cells will not respond to BLS.

These data suggest that selective stimulation of the enteric cholinergic system alleviates intestinal inflammation and provides potential therapeutic benefit in a murine model of acute colitis.
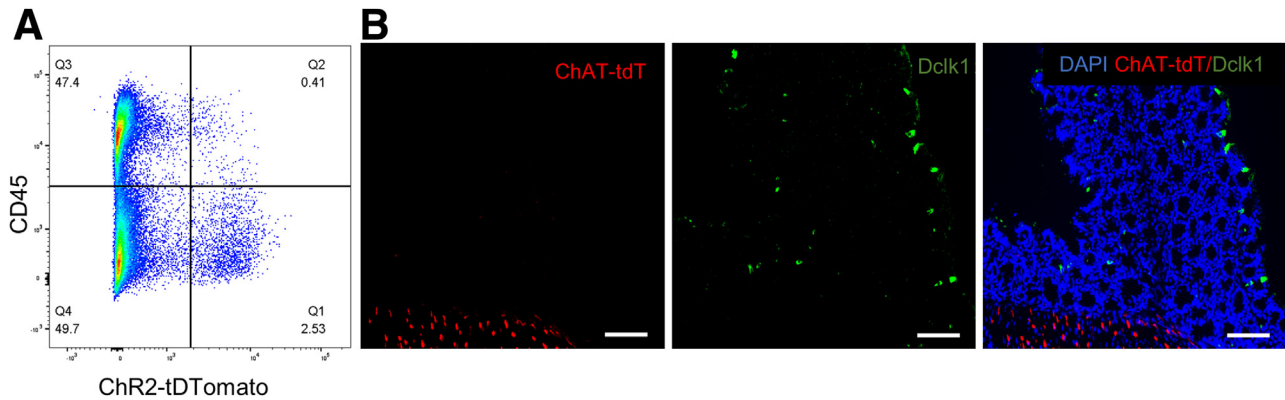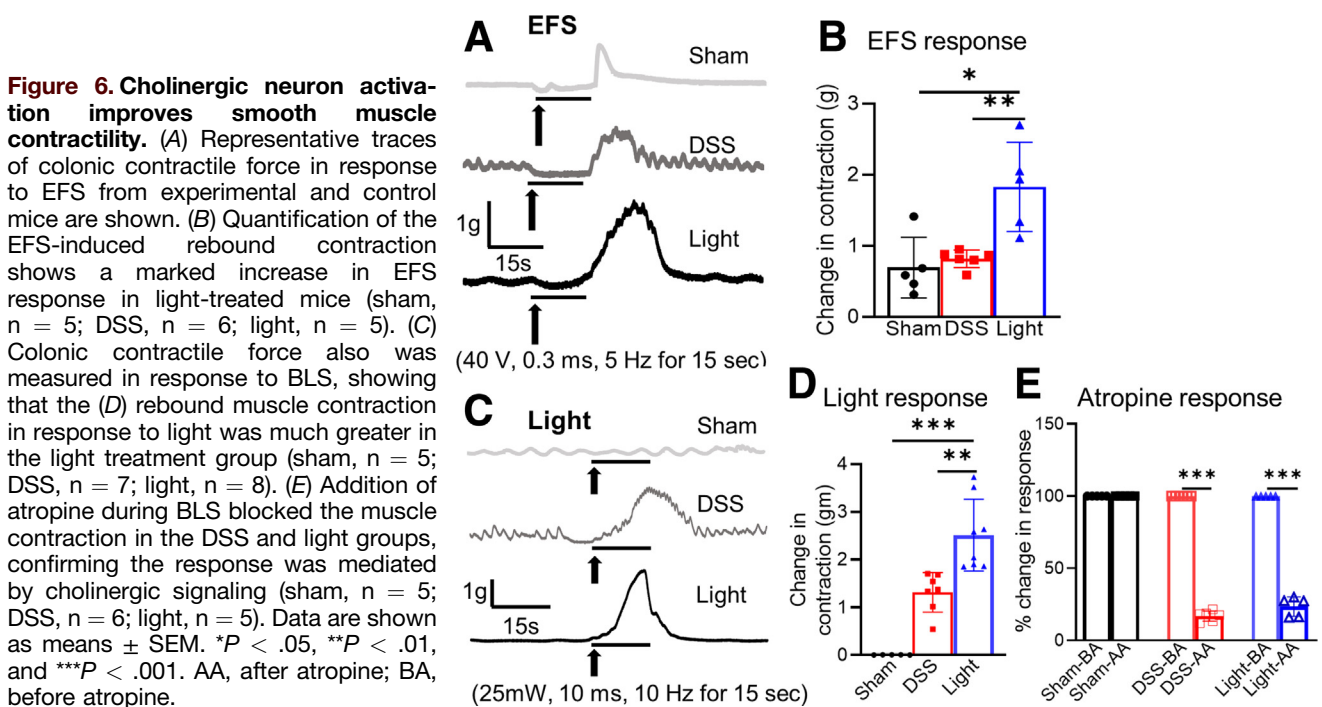
Figure 5. Non-neuronal cell expression of ChAT. (*A*) Representative flow cytometry pseudocolor plot of tdT and CD45 expression in live colonic cells from ChAT-ChR2 mice after administration of DSS for 7 days. $CD45^+$ hematopoietic cells that co-expressed tdT, which marks ChAT expression, constituted only 0.41% of all live colonic cells (second quartile, Q2), whereas nonhematopoietic tdT^+ cells constituted 2.53% of all live cells (first quartile, Q1). (*B*) Immunohistochemical labeling with tuft cell marker (Dclk1) in cross-sections of the colon of ChAT-TdT mice. *Scale bars*: 100 μm.
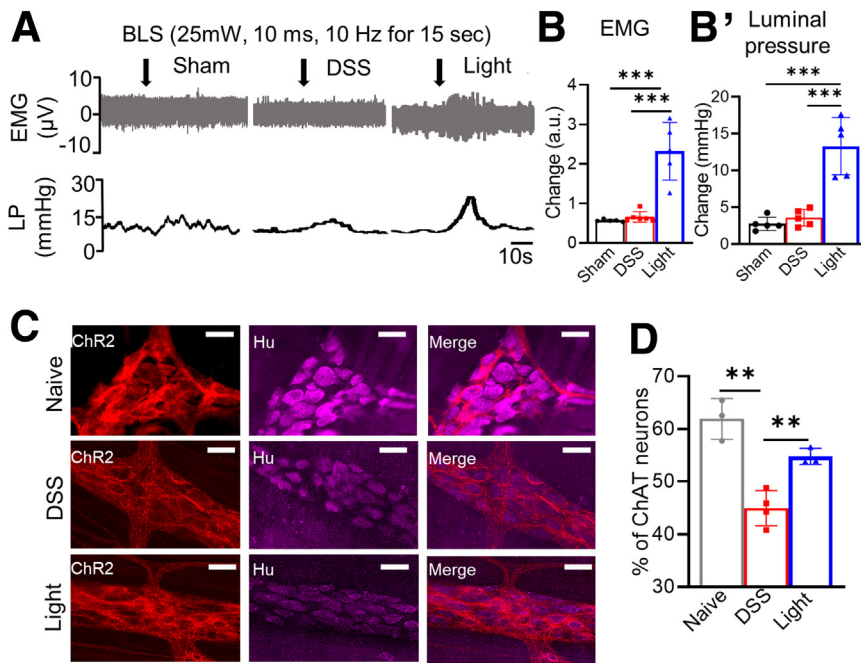
Optogenetic Activation of Cholinergic Neurons Restores Smooth Muscle Contractility

Although colitis is known to be associated with a reduction of smooth muscle contractility, light-mediated activation of cholinergic neurons restored colonic contractility in DSS-treated mice, as indicated by an increase in EFS-induced rebound contraction (1.8 ± 0.3 vs 0.8 ± 0.1 g; $P <$ .01) compared with DSS alone (Figure 6*A* and *B*). This was confirmed by BLS of the serosal surface of the colon, with significantly greater contractility in the light-treated group (2.5 ± 0.3 vs 1.3 ± 0.2 g; $P <$ .01) (Figure 6*C* and *D*). Again, this effect was abrogated by addition of atropine (Figure 6*E*), confirming that it is dependent on cholinergic signaling.

Optogenetic Activation of Cholinergic Neurons Improves Colonic Motility and Reduces Cholinergic Neuronal Loss Owing to Colitis

Effects of cholinergic neurons on colonic motility were assessed by recording electromyography (EMG) and luminal pressure (Figure 7*A*, *B*, and *B'*). DSS treatment led to a blunted response to EMG (Figure 7*B*) and a minimal change in luminal pressure (Figure 7*B'*) after BLS. However, light treatment in mice with ChAT-ChR2$^+$ neurons significantly increased EMG activity (2.3 ± 0.3 arbitrary unit (a.u.); $P <$ .001) (Figure 7*A* and *B*) and luminal pressure (13 ± 1.7 mm Hg; $P <$ .01) (Figure 7*A* and *B'*). Immunohistochemistry was performed to assess for potential loss of cholinergic neurons resulting from colitis. Although the percentage of ChAT

Figure 6. Cholinergic neuron activation improves smooth muscle contractility. (*A*) Representative traces of colonic contractile force in response to EFS from experimental and control mice are shown. (*B*) Quantification of the EFS-induced rebound contraction shows a marked increase in EFS response in light-treated mice (sham, n = 5; DSS, n = 6; light, n = 5). (*C*) Colonic contractile force also was measured in response to BLS, showing that the (*D*) rebound muscle contraction in response to light was much greater in the light treatment group (sham, n = 5; DSS, n = 7; light, n = 8). (*E*) Addition of atropine during BLS blocked the muscle contraction in the DSS and light groups, confirming the response was mediated by cholinergic signaling (sham, n = 5; DSS, n = 6; light, n = 5). Data are shown as means ± SEM. *$P <$ .05, **$P <$ .01, and ***$P <$ .001. AA, after atropine; BA, before atropine.

Figure 7. Cholinergic activation improves colonic motor activity and attenuates loss of ChAT neurons in DSS colitis. (*A*) Representative traces of EMG and luminal pressure recordings are shown (*scale bar*: 10 seconds), with significant increases in both observed in (*B*) EMG in the light-treated group (sham, n = 5; DSS, n = 6; light, n = 5) and in the (*B'*) luminal pressure in the light-treated group (n = 5 per group). (*C* and *D*) The proportion of cholinergic neurons (ChR2+) relative to total myenteric neurons (Hu) was quantified using whole mount immunofluorescence (sham, n = 3; DSS, n = 4; light, n = 3). *Scale bar*: 50 μm. Data are shown as means $\pm$ SEM. **P < .01, and ***P < .001. LP, luminal pressure.

neurons relative to the total number of Hu+ enteric neurons was reduced in DSS-induced colitis (44.9% $\pm$ 1.7% vs 61.9% $\pm$ 2.2%; P < .01), concurrent BLS attenuated the loss of cholinergic enteric neurons (54.8% $\pm$ 0.9%; P < .01) (Figure 7*C* and *D*).

ACh Reduces Cytokine Release From Resident Muscularis Macrophages In Vitro

Based on the known role of macrophages in mediating the systemic cholinergic anti-inflammatory pathway, we examined the role of ACh on the inflammatory state of resident muscularis macrophages in the colon. This was performed using transgenic mice with green fluorescent protein expressed by C-X3-C motif chemokine receptor 1 and red fluorescent protein expressed by C–C chemokine receptor 2 (Cx3cr1^{GFP};CCR2^{RFP}) mice. Single-cell suspensions were generated from the muscularis propria of the colon. Cx3cr1^{GFP} macrophages were isolated by flow cytometry (Figure 8*A*) and cultured *in vitro* in media containing colony stimulating factor 1 (CSF-1) (Figure 8*B*). Exposure of cultured macrophages to lipopolysaccharide (LPS) in vitro significantly up-regulated the expression of *Tnf* more than 300-fold, and this was reduced significantly by addition of ACh in a dose-dependent manner (Figure 8*C*). These results show that ACh can act directly on resident macrophages and reduce their inflammatory response. To determine whether enteric cholinergic neurons are capable of exerting an anti-inflammatory effect, we performed a co-culture experiment in which muscularis macrophages were cultured with enteric cholinergic neurons expressing channelrhodopsin. Addition of LPS to the cultures led to interleukin (IL)1β expression by CD11b-expressing macrophages, but not by the neurons (Figure 8*D*). Activation

of ChAT-expressing neurons with BLS led to a significant reduction in IL1β expression by the muscularis macrophages, supporting the anti-inflammatory role of enteric cholinergic neurons (Figure 8*E*).

Discussion

In the present study, we report that cholinergic enteric neurons, intrinsic to the intestine, play an important role in modulating the severity of colitis. Local ablation of cholinergic enteric neurons exacerbates DSS-induced experimental colitis, whereas optogenetic activation of this neuronal subpopulation exerts a protective, anti-inflammatory effect. Activation of cholinergic neurons also restores colonic contractility, which normally is disrupted in the setting of colitis. Although extrinsic cholinergic signaling is known to have a systemic anti-inflammatory role,[10–12] the morphologic and functional improvements we observed in response to local optogenetic activation of the distal colon suggest an important immunoregulatory role for the intrinsic ChAT-expressing neurons of the ENS.

There is ample evidence supporting a direct effect of intestinal inflammation on enteric neurons. Both clinical and experimental models of IBD are associated with disruption of the enteric neuronal network, both structurally and functionally. This includes loss of enteric neurons, axonal degeneration, neuronal hyperexcitability, altered neurotransmission, and changes to the neurochemical coding of myenteric neurons, especially affecting the cholinergic and nitrergic subpopulations.[24–30] Recently, it was shown that ACh levels are reduced in the colons of patients with IBD and in mice with colitis.[22] Because the intrinsic cholinergic neurons are anti-inflammatory, as our data showed, then their loss or injury in the setting of inflammation potentially
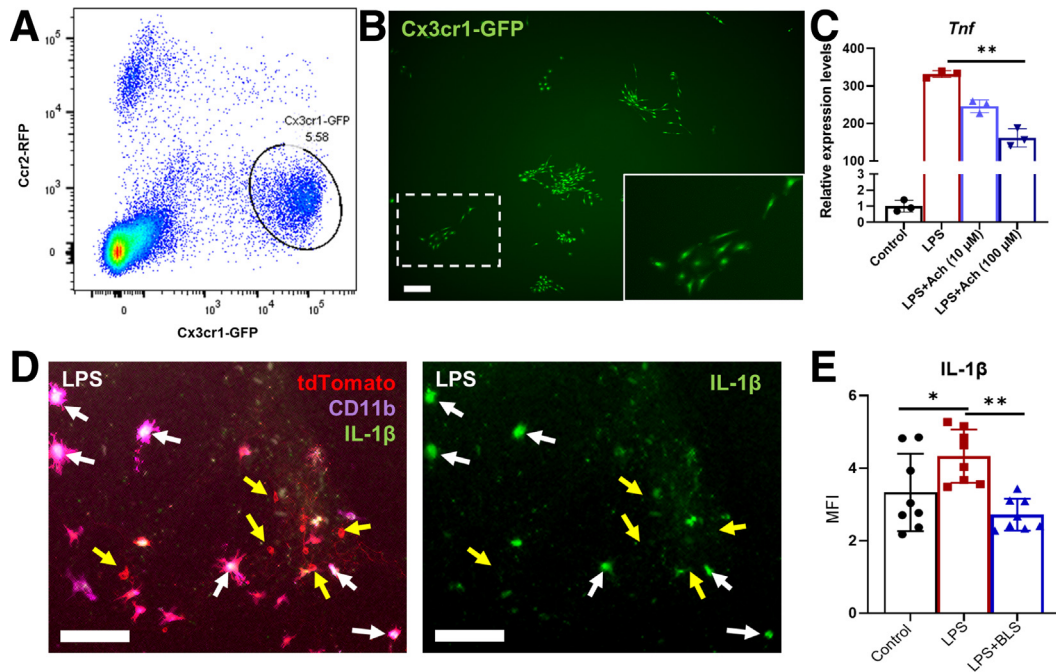
Figure 8. ACh reduces cytokine release from cultured resident macrophages. (*A*) GFP-expressing macrophages were isolated by flow cytometry from the colonic muscularis propria of Cx3cr1^{GFP};CCR2^{RFP} mice. (*B*) Cx3cr1^{GFP} macrophages were cultured in vitro and formed colonies in the presence of CSF-1 (*dashed box* enlarged in *inset*). (*C*) Transcript levels of *Tnf* in the presence of LPS (100 ng/mL) were reduced significantly by the addition of ACh in a dose-dependent manner (n = 3 per group). Channelrhodopsin-expressing cholinergic neurons (ChAT$^{ChR2-tdT}$) and muscularis macrophages (Cx3cr1^{tdT}) were co-cultured in vitro. (*D*) After addition of LPS, IL1β can be seen expressed by tdT+/CD11b+ macrophages (*white arrows*), and not by tdT+/CD11b-negative cholinergic neurons (*yellow arrows*). (*E*) Quantification of IL1β immunofluorescence (MFI, mean fluorescence intensity) is shown in control conditions, in the presence of LPS, and with LPS after BLS to activate ChAT-expressing neurons (n = 8 per group). *Scale bars*: 200 μm (*B*), 50 μm (*D*). Data are shown as means ± SEM. **$P < .01$, *$P < .05$.

could exacerbate the underlying colitis. This may offer one possible explanation for the progression of disease in IBD. We therefore propose that protecting and/or enhancing cholinergic innervation in the gut may be an effective and novel treatment strategy for IBD.

Conventional therapies for IBD often are associated with significant morbidity and do not induce durable remission. The development of safe, targeted, and long-lasting therapies is needed. The reciprocal relationship between colitis and the ENS, particularly with respect to the cholinergic system, suggests that preventing cholinergic neuronal damage or dysfunction can reduce inflammation in IBD. The well-known systemic CAIP represents a neurally mediated immunoregulatory pathway in which activation of the vagus nerve inhibits cytokine release via α7nAChRs present on macrophages.[13] This anti-inflammatory signaling pathway has been suggested as a potential therapeutic target for the treatment of various diseases, including autoimmune disorders[31] and coronavirus disease-2019.[32] With respect to GI pathologies, the vagus nerve likely activates α7nAChR indirectly, given that vagal efferents are not in physical contact with resident muscularis macrophages in the gut. Instead, neuroanatomic studies have shown that the vagus nerve interacts with cholinergic myenteric neurons in the intestine, which then project their nerve endings in close proximity to muscularis macrophages,[18,33] suggesting an important intermediary role for enteric neurons in the

gastrointestinal CAIP. In a model of postoperative ileus, Kalff et al[34] found that resident muscularis macrophages were increased markedly in number and adopted an activated phenotype after bowel manipulation, and the degree of myeloid infiltration in the muscularis correlated with both the extent of manipulation and subsequent impairment in bowel contractility. Taken together with the findings by The et al[12] that preoperative vagal nerve stimulation or administration of an α7 nicotinic receptor agonist prevented the development of postoperative ileus and attenuated immune cell infiltration in the muscularis, this suggests a critical interplay between cholinergic signaling, muscularis macrophages, and gut motility.

Our results using optogenetic activation of cholinergic signaling are consistent with the recent finding that local administration of ACh by enema attenuates DSS-induced colitis.[22] Moreover, we found that activation of cholinergic enteric neurons protects against their loss due to inflammation. Finally, we showed that cholinergic activation led to down-regulation of proinflammatory cytokines, including *Il1b*, *Il6*, and *Il17a*, and that treatment of muscularis macrophages with ACh similarly reduced the production of proinflammatory cytokines. Although intestinal muscularis macrophages have been shown to express the α7 nicotinic ACh receptor by immunohistochemistry and flow cytometry, studies of intestinal inflammation and the CAIP have been limited to the use of macrophages from other sources (such

as the peritoneal cavity and spleen) for in vitro studies and the findings then generalized to resident intestinal muscularis macrophages.[11,12,35] By using cultured muscularis macrophages isolated from the colon, we show that ACh itself, as well as optogenetic activation of enteric cholinergic neurons, exerts an anti-inflammatory effect on resident muscularis macrophages, confirming the important immunoregulatory role of these neurons in the gut.

One limitation of this study was the possibility that other ChAT-expressing cells in the gut, such as T cells, B cells,[36] and tuft cells,[37] in addition to enteric cholinergic neurons, may have been activated by BLS in our model. These other ChAT+ cells, however, are found in relatively small numbers in the colon.[38] Using flow cytometry, we found that hematopoietic (CD45+) cells that co-expressed tdT (a marker of ChAT expression) constituted only 0.4% of live cells, whereas tdT+ nonhematopoietic (CD45-) cells (which we presume to be enteric cholinergic neurons and tuft cells) constituted 2.5% of cells (Figure 5A). Although tuft cells have been shown to express ChAT in the respiratory system,[39] we did not find ChAT expression by colonic tuft cells in our model (Figure 5B). One explanation for this may be that ACh in tuft cells can be catalyzed by the enzyme carnitine acetyltransferase, rather than ChAT.[37,40] We conclude that even if ChAT+ CD45+ hematopoietic cells were activated by BLS, given their low numbers, they are unlikely to explain the therapeutic effect we observed. In addition, it is not known what effect optogenetic activation of the ChR2 channel and subsequent influx of cations would have on immune cells, whereas the excitatory effect of ChR2 activation in neurons is well described.[41] However, further studies are needed to test whether activation of immune cells may have a protective, anti-inflammatory effect in colitis.

Elucidating the anti-inflammatory mechanism of cholinergic activation on colitis requires additional investigation. For example, activation of cholinergic neurons improved colonic smooth muscle contractility and decreased loss of ChAT-expressing neurons, but it is unknown whether this occurred owing to an overall decrease in inflammation or to the excitatory effect of ACh on intestinal smooth muscle. Second, we examined the effects of ACh on muscularis macrophages, which are particularly pertinent to the onset of dysmotility as established in studies of postoperative ileus,[34] but the relationship between enteric cholinergic neurons and monocytes and macrophages in the mucosa and submucosa warrants exploration. Additionally, this study was performed using an acute colitis model. Studies of optogenetic cholinergic neuron stimulation in a model of chronic colitis will be important to determine whether cholinergic enteric signaling can suppress inflammation and induce remission in chronic inflammation as occurs in human IBD. Finally, we applied optogenetic activation during DSS treatment. From a translational perspective, we need to determine whether cholinergic activation not only can prevent, but also treat, colitis.

In conclusion, we have shown that a reduction in enteric cholinergic neurons aggravates inflammation and abolishes smooth muscle contractility in colitis. Conversely, targeted stimulation of enteric cholinergic neurons reduces inflammation, preserves motility and smooth muscle contractility, and protects against cholinergic enteric neuronal loss. Together, these findings highlight the integral role of enteric cholinergic neurons in neuroimmune regulation, and suggest that interventions to restore damaged cholinergic neurons or locally activate enteric cholinergic signaling may represent novel approaches to complement current treatments for IBD.

Methods
Animals

All animal protocols were approved by the Institutional Animal Care and Use Committee at Massachusetts General Hospital (protocols #2009N000239 and #2013N000115). All methods were performed in accordance with relevant regulations. The following mouse lines were obtained from Jackson Laboratory (Bar Harbor, ME): *ChAT::Cre* mice (stock #006410) were crossed with *R26-iDTR* mice (stock #007900) to obtain *ChAT::Cre;R26-iDTR* (annotated as ChAT-iDTR) mice. *ChAT::Cre* mice also were crossed with *R26-ChR2-tdTomato* (stock #012567) reporter mice to obtain *ChAT::Cre;R26-ChR2-tdTomato* (annotated as ChAT-ChR2) mice, in which ChAT+ cells express the light-sensitive ion channel ChR2 and red fluorescent protein, tdT. Cx3cr1GFP;CCR2RFP mice (stock #032127), in which red fluorescent protein is expressed by peripheral monocytes and lymphocytes, and green fluorescent protein is expressed by macrophages. All experiments used adult mice (both sexes) between 10 and 12 weeks of age.

Induction of Colitis

A DSS-induced colitis model, which has been widely used because of its comparable clinical, immunologic, and histologic features with ulcerative colitis,[42] was used. To induce colitis, mice were treated with 2.5% DSS (cat# 160110; MP Biomedicals) in the drinking water for 7 days.

Cholinergic Neuron Ablation

To determine the role of enteric cholinergic neurons in colonic inflammation, ablation of ChAT-expressing neurons was achieved using ChAT-iDTR mice, in which ChAT+ neurons express the receptor for human DT (#D0564; Sigma Aldrich, St. Louis, MO). Focal injection of 4 μL of 1 ng/μL DT into the midcolon of ChAT-iDTR mice lead to selective ablation of cholinergic neurons in the myenteric plexus, with preservation of enteric neurons surrounding the injection site, as we showed previously in Wnt1-iDTR mice.[43] These DT-injected mice were treated with 2.5% DSS in the drinking water for 7 days to induce colitis, representing the ablated experimental group. ChAT-iDTR mice that did not receive DSS or DT served as naïve controls. The DSS group consisted of Cre-negative mice, in which ChAT+ neurons do not express the receptor for DT, also were treated with both DSS and DT injection (Figure 1A).

Blue Light Stimulation of Cholinergic Neurons

Under general anesthesia, BLS was applied through a diode-pumped, solid-state laser system (470 nm, 200 mW, model: MDL-III-470; OptoEngine, LLC, Midvale, UT) using a 3-cm–long rectal optogenetic probe (Prizmatix) inserted through the rectum and projecting to the distal colon. BLS was administered daily for 7 days. The light was delivered over 30 minutes, cycling between 10 seconds of illumination with 10-ms pulses at 10 Hz, followed by 20 seconds off. These mice were compared with a sham group, in which DSS and BLS were administered to Cre-negative mice (which do not express ChR2 and thus will not undergo neuronal activation in response to BLS).

Immunohistochemistry

Immunohistochemistry was performed as previously described.[44,45] Whole mount preparations of the longitudinal muscle myenteric plexus and full-thickness colon samples were fixed in 4% paraformaldehyde. For cryosections, full-thickness colon samples were dehydrated in 15% sucrose at 4°C overnight, then incubated in 15% sucrose with 7.5% gelatin at 37°C for 1 hour and snap frozen at −80°C and sectioned at 12 μm with a CM3050 S cryostat (Leica, Buffalo Grove, IL). Both whole mount longitudinal muscle myenteric plexus and cryostat cross-sections were permeabilized with 0.1% Triton X-100 and blocked with 10% donkey serum. Primary antibodies included anti-human HuC/D (Anti-neuronal nuclear antibody (ANNA-1), goat, 1:16000, kindly gifted by the Lennon Laboratory, Mayo Clinic), anti-CD45 (rat, 1:500; BioLegend), anti-VAChT (goat, 1:500; Millipore), anti-nNOS (rabbit, 1:200; ThermoFisher), and anti-Dclk1 (rabbit, 1:500; Abcam). Anti-HuC/D antibody is a widely used pan-neuronal marker, labeling the neuronal cell body[46]; anti-CD45 antibody is a pan-leukocyte marker; anti-VAChT antibody identifies cholinergic neuronal fibers[47,48]; and anti-Dclk1 is the most widely used tuft cell marker and 95% of Dclk1+ epithelial cells in the murine intestine are tuft cells.[49] Secondary antibodies included anti-human IgG (1:200, Alexa Fluor 647; Fisher Scientific Life Technologies), anti-goat IgG (1:500, Alexa Fluor 488; Fisher Scientific Life Technologies), anti-rabbit IgG (1:500, Alexa Fluor 488 and 546; Fisher Scientific Life Technologies), and anti-rat IgG (1:500, Alexa Fluor 488; Fisher Scientific Life Technologies). Cell nuclei were counterstained with 4′,6-diamidino-2-phenylindole (DAPI) (Vector Labs, Burlingame, CA) and mounted with Aqua-Poly/Mount (Fisher Scientific Polysciences, Inc). Images were obtained with a Nikon A1R laser scanning confocal microscope (Nikon Instruments, Melville, NY) or a Keyence BZX-700 All-In-One microscope (Keyence America, Itasca, IL).

Histology

After fixation, tissues were paraffin-embedded, sectioned at 5 μm, deparaffinized, cleared, and rehydrated in graded ethanol solutions. For standard H&E staining, sections were immersed in xylene (3 × 4 min), 100% ethanol (3 min), 90% ethanol (2 min), 70% ethanol (2 min), and rinsed in tap water. They then were immersed in hematoxylin (4 min), and rinsed in tap water, Scott's tap water (1 minute), eosin (3 minutes), and again rinsed in tap water. This was followed by incubation in 100% ethanol (2 × 1 min), xylene (2 × 3 min), and mounting on glass slides with distyrene plasticizer xylene mountant.

Assessment of Inflammation

To assess the severity of colonic inflammation, fecal Lcn-2 and gross morphologic injury were quantified. Lcn-2, also known as neutrophil gelatinase-associated lipocalin, is a sensitive noninvasive biomarker of intestinal inflammation[50] and was quantified by enzyme-linked immunosorbent assay, as previously described.[21] Fecal samples were collected from mice daily for 7 days. Briefly, fecal samples were reconstituted in phosphate-buffered saline (PBS)–0.1% Tween 20 (100 mg/mL) and vortexed for 20 minutes to form homogenous fecal suspensions. Samples then were centrifuged for 10 minutes at 12,000 rpm and 4°C. Lcn-2 levels were quantified in the supernatants using a Duoset murine Lcn-2 enzyme-linked immunosorbent assay kit (R&D Systems, Minneapolis, MN). Gross morphologic damage in H&E-stained colonic sections was assessed by histologic grading of 8 parameters.[51] Leukocyte infiltration (0–3), goblet cell loss (0–3), crypt density (0–3), crypt hyperplasia (0–3), muscle thickening (0–3), submucosal inflammation (0–3), crypt abscesses (0 –3), and ulceration (0–3) (average of 8 areas of 500 μm^2 per animal). Quantitative analyses were conducted blindly.

Quantitative Analyses of Immunohistochemical, Histologic, and Morphologic Data

The total number of myenteric neurons immunoreactive for Hu and VAChT/ChR2 (tdTomato) were quantified in whole mount preparations within a 2 mm^2 area by randomly capturing 8 images per preparation at 20× magnification. Leukocyte infiltration into the colonic wall was assessed by counting the total number of CD45 immunoreactive cells within the mucosal and muscular layers in cross-sections (total area, 1.5 mm^2). All images were captured under identical acquisition exposure time conditions and calibrated to standardized minimum baseline fluorescence. Images were converted from red, green, and blue to grayscale 8 bit, then further processed to binary images, with changes in fluorescence from baseline measured using ImageJ software (National Institutes of Health, Bethesda, MD).

Determination of mRNA Expression in Colonic Tissue

mRNA was extracted from snap-frozen colonic tissue. Homogenization of the samples was performed using 500 μL TRIzol reagent at 4°C (#15596018; Invitrogen, Thermo Fisher Scientific, Waltham, MA). RNA isolation was performed with RNEasy kits (Qiagen) and quantified using the Qubit RNA HS Assay Kit (Invitrogen, Thermo Fisher Scientific) on a Qubit 4 Fluorometer (Invitrogen, Thermo Fisher Scientific).

Quantitative Polymerase Chain Reaction

Total RNA was reverse-transcribed and amplified via reverse-transcription quantitative polymerase chain reaction (PCR) with the iTaq Universal SYBR Green One-Step Kit (Bio-Rad, Hercules, CA) using a Bio-Rad CFX96 real-time thermal cycler. Glyceraldehyde-3-phosphate dehydrogenase (Gapdh) was amplified using the primer sequences AGGTCGGTGTGAACGGATTTG (forward) and TGTAGACCATGTAGTTGAGGTCA (reverse). Tumor necrosis factor-α was amplified using the primer sequences CCTCT TCTCATTCCTGCTTGT (forward) and TGGGAACTT CTCATCCCTTTG (reverse). IL6 was amplified using the primer sequences GATACCACTCCCAACAGACC (forward) and CAAGTGCATCATCGTTGTTCA (reverse). Il17 was amplified using the primer sequences TTTAACTCCC TTGGCGCAAAA (forward) and CTTTCCCTCCGCATTGACAC (reverse). Ilb was amplified using the primer sequences GACCTGTTCTTTGAAGTTGACG (forward) and CTCTTGTT GATGTGCTGCTG (reverse). ChAT was amplified using the primer sequences GAGCGAATCGTTGGTATGACAA (forward) and AGGACGATGCCATCAAAAGG (reverse). Protein tyrosine phosphatase receptor type C (Ptprc) was amplified using the primer sequences GTTTTCGCTACATGACTGCACA (forward) and AGGTTGTCCAACTGACATCTTTC (reverse). Lymphocyte antigen 6 family member G (Ly6g) was amplified using the primer sequences GACTTCCTGCAACACAACTACC (forward) and ACAGCATTACCAGTGATCTCAGT (reverse). Results were processed using Bio-Rad CFX Manager software (version 3.1), with a standard threshold to quantify cross point (Ct) values. Ct values for tumor necrosis factor-α, IL6, IL17a, IL1B, ChAT, Ptprc, and Ly6g were normalized to Gapdh. All reactions were performed in duplicate.

Flow Cytometry

Mice were killed and the colons were isolated for digestion to a single-cell suspension. Full-thickness colon (containing mucosa, submucosa, and muscularis propria) was minced and incubated in collagenase XI (1 mg mL^{-1}; Sigma Aldrich) and dispase (250 μg mL^{-1}; STEMCELL Technologies, Vancouver, Canada) for 60 minutes at 37°C to generate single-cell suspensions. Samples were then centrifuged at 500g for 5 minutes, the supernatant aspirated, the pellet resuspended in PBS-2% FBS (Thermo-Fisher, Gibco, 10438-018), and the suspension passed through a 40 μmol/L sterile cell strainer (Fisher Scientific, #22363547) twice. Samples were incubated with anti-mouse CD45 antibody (1:00, Alexa Fluor 488; BioLegend) in PBS-2% FBS for 30 minutes at room temperature, washed 3 times with PBS-2% FBS, and resuspended in PBS-2% FBS with DAPI (1:300; Vector Labs) as a marker of cell viability immediately before analysis. Flow cytometry of stained samples then was performed with a BD FACSAria cell sorter (BD Biosciences) and the data analyzed with FlowJo software (FlowJo, LLC, OR).

Organ Bath Smooth Muscle Activity Studies

Standard organ bath techniques have been described previously.[45,46] Briefly, freshly excised distal colon was quickly placed in Krebs solution. Tissue was cut into 5-mm rings and mounted between 2 small metal hooks attached to force displacement transducers in a muscle strip myograph bath (Model 820 MS; Danish Myo Technology, Aarhus, Denmark) containing oxygenated Krebs solution at 37°C. The rings were gently stretched to deliver a basal tension of 0.5 g and were equilibrated for 60 minutes, with the Krebs changed every 20 minutes.

For EFS, colon segments were then stimulated with pulse trains of 40 V for 15 seconds, with pulse duration of 300 μs, at a frequency of 5 Hz using a CS4+ constant voltage stimulator with Myo Pulse software (Danish Myo Technology, Aarhus, Denmark). Force contraction of the circular smooth muscle was recorded and analyzed using a Power Lab 16/35 data acquisition system (ADInstruments, NSW, Australia) and Lab Chart Pro Software v8.1.16 (ADInstruments). Acetylcholine (ACh, 100 μmol/L; Sigma) was added to the organ bath to measure maximum contraction and atropine (1 μmol/L; Sigma) was added to block cholinergic transmission. Tissue viability and integrity were confirmed at the end of the experiment by measuring contraction response to 60 mmol/L KCl.

BLS was applied from a diode-pumped solid-state laser system (470 nm, 200 mW, model: MDL-III-470; OptoEngine, LLC, Midvale, UT). Trains of light pulses (10-ms pulse width, 10 Hz, 15-second train duration) were shined focally on the serosal surface of the colon in the organ bath via an optic fiber (diameter, 200 μm).

In Vivo EMG and Luminal Pressure Measurement

General anesthesia was induced with isoflurane and normothermia was maintained by placing mice on a heating pad. A 3- to 4-cm laparotomy incision was made, and the colon exposed. A cannula connected to a saline filled syringe with a stopcock was inserted 2-cm distal to the cecum and suture ligated in place. The colon was flushed with saline to remove all enteric contents and ligated distally to establish a closed system. The proximal canula was connected to a pressure transducer (CWE, Inc, Ardmore, PA), which converts luminal pressure to an analogue signal. The colon was filled with saline to a set pressure of 10–15 mm Hg. EMG was recorded with 2 sets of custom made 3-lead needle electrodes (Motion Lab Systems, Inc, Los Angeles, CA) positioned on the muscle layer of the mid- to distal colon. The electrodes were connected to a four channel Bio-amplifier (CWE, Inc) through an ISO-Z Isolated Head Stage amplifier (CWE, Inc). EMG and luminal pressure signals were digitized and recorded using a Power Lab 16/35 data acquisition system (ADInstruments, New South Wales, Australia) and analyzed with Lab Chart Pro Software v8.1.16 (ADInstruments).

In Vitro Macrophage Culture

Cx3cr1^{GFP};CCR2^{RFP} mice were killed and colons were excised for the generation of single-cell suspensions from the muscularis propria as previously described.[52] Briefly, after removing the mucosa/submucosa, the muscularis propria layer was minced and then incubated in collagenase XI (1 mg mL^{-1}; Sigma Aldrich, St. Louis, Missouri) and dispase (250 μg mL^{-1}; STEMCELL Technologies) for 45

minutes to generate single-cell suspensions. Fluorescent-activated cell sorting (FACS) was conducted using a BD FACSAria cell sorter (BD Biosciences, Franklin Lakes, NJ) to isolate Cx3cr1^{GFP} macrophages. Analysis of FACS data was performed using FlowJo software (FlowJo, LLC). Cells were seeded into 24-well fibronectin (#F1141; Sigma)-coated plates containing macrophage expansion media (RPMI1640 media [R8758; Sigma], 10% fetal bovine serum [FBS] [10438-018; ThermoFisher, Gibco], 1% penicillin-streptomycin [15140122; ThermoFisher, Gibco], and 10 ng/mL recombinant mouse monocyte-macrophage colony stimulating factor (M-CSF) [#576404; BioLegend]) at a density of 2×10^4 cells/well. Cultures were incubated for 14 days with the media replaced every 2–3 days. To activate macrophages, cultures were exposed to 100 ng/mL of LPS (#L2880; Sigma) for 2 hours. To assess the effects of ACh, 10–100 μmol/L of ACh (A6625; Sigma) was applied with LPS in the presence of 100 μmol/L pyridostigmine bromide (P9797-1G; Sigma). Total RNA was extracted using the RNeasy Mini kit (#74106; Qiagen) as previously described,[53] and reverse-transcription quantitative PCR was performed with the iTaq Universal SYBR Green One-Step Kit (Bio-Rad, Hercules, CA) using a Bio-Rad CFX96 cycler.

In Vitro Co-Culture of Enteric Neurons and Intestinal Muscularis Macrophages

Muscularis propria was collected from euthanized Cx3cr1CreERT2-tdT mice and digested at 37°C for 45 minutes in collagenase XI (1 mg mL−1; Sigma Aldrich) and dispase (250 μg mL−1; STEMCELL Technologies). The single-cell suspension was filtered through a Cell Strainer Snap Cap (#352235; Corning). tdTomato-positive cells were collected by FACS using a BD FACSAria cell sorter. A total of 6×10^3 Tdt-positive cells/well were seeded into a 48-well plate (#353078; FALCON), fibronectin-coated (#F1141; Sigma), and cultured in complete media as described earlier for 1 week. To isolate enteric neurospheres for co-culture, the muscularis propria of colon from ChAT-ChR2 mice was digested enzymatically as described previously.46 Co-culture of the enteric neurospheres and muscularis macrophages was conducted in complete media including 50% RPMI1640 (#R8758; Sigma), 50% NeuroCult Basal Media, 10% FBS (#10438-018; ThermoFisher, Gibco), 1% penicillin-streptomycin (15140122; ThermoFisher, Gibco), and 10 ng/mL recombinant mouse M-CSF (#576404; BioLegend) for 6 days. Samples were exposed to 100 ng/mL LPS with 100 μmol/L pyridostigmine bromide for 2 hours, and BLS was applied to each well. The light was delivered over 30 minutes, cycling between 10 seconds of illumination with 10-ms pulses at 10 Hz, followed by 20 seconds off using an optic fiber (diameter, 200 μm) placed on the liquid surface of each well.

Immunohistochemistry for In Vitro Cultures

Co-cultures of enteric neurons and muscularis macrophages were fixed with 4% Paraformaldehyde (PFA) solution (#15710; Electron Microscopy Science). The samples were blocked and permeabilized in 10% donkey serum (#D9663; Sigma), 0.1% Triton in PBS. Primary antibodies were incubated in PBS containing 2% donkey serum and 0.1% Triton (Sigma Aldrich, Cat. #X-100) at 4°C overnight, followed by secondary antibody for 1 hour at room temperature and stained with DAPI (#D1306; Invitrogen) for 5 minutes. Primary antibodies used in this study included CD11b (#101212, 1:200; BioLegend) and IL1β (ab254360, 1:200; Abcam). Secondary antibody donkey anti-rabbit 488 (A21206, 1:200; Invitrogen) on a Keyence BZX-700 All-In-One Microscopy system, and the fluorescence of IL1β in muscularis macrophages, was quantified by ImageJ in a 10 mm2 area from each sample.

Statistical Analysis

Grouped data are expressed as means ± SEM. Statistical analysis was conducted with GraphPad Prism (version 9; Graphpad Software, Inc, San Diego, CA). An unpaired t test was used to analyze peak effects, and parametric data were analyzed by 1-way analysis of variance followed by the Bonferroni test for multiple group comparisons. For reverse-transcription quantitative PCR data, the mRNA level of each gene was normalized to Gapdh and expressed using the $2^{-\Delta\Delta Ct}$ method.[54] For all comparisons, $P < .05$ was considered statistically significant.

References

1. Plichta DR, Graham DB, Subramanian S, et al. Therapeutic opportunities in inflammatory bowel disease: mechanistic dissection of host-microbiome relationships. Cell 2019;178:1041–1056.
2. Dahlhamer JM, Zammitti EP, Ward BW, et al. Prevalence of inflammatory bowel disease among adults aged ≥18 years - United States, 2015. MMWR Morb Mortal Wkly Rep 2016;65:1166–1169.
3. Oka A, Sartor RB. Microbial-based and microbial-targeted therapies for inflammatory bowel diseases. Dig Dis Sci 2020;65:757–788.
4. Kuenzig ME, Fung SG, Marderfeld L, et al. Twenty-first century trends in the global epidemiology of pediatric-onset inflammatory bowel disease: systematic review. Gastroenterology 2022;162:1147–1159.e4.
5. Lewis RT, Maron DJ. Efficacy and complications of surgery for Crohn's disease. Gastroenterol Hepatol (N Y) 2010;6:587–596.
6. Furness JB. The enteric nervous system and neuro-gastroenterology. Nat Rev Gastroenterol Hepatol 2012; 9:286–294.
7. Mawe GM, Strong DS, Sharkey KA. Plasticity of enteric nerve functions in the inflamed and postinflamed gut. Neurogastroenterol Motil 2009;21:481–491.
8. Lindgren S, Stewenius J, Sjölund K, et al. Autonomic vagal nerve dysfunction in patients with ulcerative colitis. Scand J Gastroenterol 1993;28:638–642.
9. Stavely R, Rahman AA, Sahakian L, et al. Divergent adaptations in autonomic nerve activity and neuroimmune signaling associated with the severity of inflammation in chronic colitis. Inflamm Bowel Dis 2022;28:1229–1243.

10. Borovikova LV, Ivanova S, Zhang M, et al. Vagus nerve stimulation attenuates the systemic inflammatory response to endotoxin. Nature 2000;405:458–462.

11. de Jonge WJ, van der Zanden EP, The FO, et al. Stimulation of the vagus nerve attenuates macrophage activation by activating the Jak2-STAT3 signaling pathway. Nat Immunol 2005;6:844–851.

12. The FO, Boeckxstaens GE, Snoek SA, et al. Activation of the cholinergic anti-inflammatory pathway ameliorates postoperative ileus in mice. Gastroenterology 2007; 133:1219–1228.

13. Wang H, Yu M, Ochani M, et al. Nicotinic acetylcholine receptor alpha7 subunit is an essential regulator of inflammation. Nature 2003;421:384–388.

14. Bonaz B, Sinniger V, Hoffmann D, et al. Chronic vagus nerve stimulation in Crohn's disease: a 6-month follow-up pilot study. Neurogastroenterol Motil 2016;28: 948–953.

15. Sinniger V, Pellissier S, Fauvelle F, et al. A 12-month pilot study outcomes of vagus nerve stimulation in Crohn's disease. Neurogastroenterol Motil 2020;32:e13911.

16. Kibleur A, Pellissier S, Sinniger V, et al. Electroencephalographic correlates of low-frequency vagus nerve stimulation therapy for Crohn's disease. Clin Neurophysiol 2018;129:1041–1046.

17. Berthoud HR, Jedrzejewska A, Powley TL. Simultaneous labeling of vagal innervation of the gut and afferent projections from the visceral forebrain with diI injected into the dorsal vagal complex in the rat. J Comp Neurol 1990;301:65–79.

18. Matteoli G, Gomez-Pinilla PJ, Nemethova A, et al. A distinct vagal anti-inflammatory pathway modulates intestinal muscularis resident macrophages independent of the spleen. Gut 2014;63:938–948.

19. Kelles A, Janssens J, Tack J. IL-1beta and IL-6 excite neurones and suppress cholinergic neurotransmission in the myenteric plexus of the guinea pig. Neurogastroenterol Motil 2000;12:531–538.

20. Poli E, Lazzaretti M, Grandi D, et al. Morphological and functional alterations of the myenteric plexus in rats with TNBS-induced colitis. Neurochem Res 2001; 26:1085–1093.

21. Robinson AM, Rahman AA, Carbone SE, et al. Alterations of colonic function in the Winnie mouse model of spontaneous chronic colitis. Am J Physiol Gastrointest Liver Physiol 2017;312:G85–G102.

22. Zheng W, Song H, Luo Z, et al. Acetylcholine ameliorates colitis by promoting IL-10 secretion of monocytic myeloid-derived suppressor cells through the nAChR/ERK pathway. Proc Natl Acad Sci U S A 2021;118: e2017762118.

23. McCann CJ, Cooper JE, Natarajan D, et al. Transplantation of enteric nervous system stem cells rescues nitric oxide synthase deficient mouse colon. Nat Commun 2017;8:15937.

24. Sanovic S, Lamb DP, Blennerhassett MG. Damage to the enteric nervous system in experimental colitis. Am J Pathol 1999;155:1051–1057.

25. Linden DR, Couvrette JM, Ciolino A, et al. Indiscriminate loss of myenteric neurones in the TNBS-inflamed

26. guinea-pig distal colon. Neurogastroenterol Motil 2005; 17:751–760.

26. Dvorak AM, Onderdonk AB, McLeod RS, et al. Axonal necrosis of enteric autonomic nerves in continent ileal pouches. Possible implications for pathogenesis of Crohn's disease. Ann Surg 1993;217:260–271.

27. Geboes K, Collins S. Structural abnormalities of the nervous system in Crohn's disease and ulcerative colitis. Neurogastroenterol Motil 1998;10:189–202.

28. Nurgali K, Nguyen TV, Matsuyama H, et al. Phenotypic changes of morphologically identified guinea-pig myenteric neurons following intestinal inflammation. J Physiol 2007;583:593–609.

29. Neunlist M, Aubert P, Toquet C, et al. Changes in chemical coding of myenteric neurones in ulcerative colitis. Gut 2003;52:84–90.

30. Winston JH, Li Q, Sarna SK. Paradoxical regulation of ChAT and nNOS expression in animal models of Crohn's colitis and ulcerative colitis. Am J Physiol Gastrointest Liver Physiol 2013;305:G295–G302.

31. Lv J, Ji X, Li Z, et al. The role of the cholinergic anti-inflammatory pathway in autoimmune rheumatic diseases. Scand J Immunol 2021;94:e13092.

32. Qin Z, Xiang K, Su DF, et al. Activation of the cholinergic anti-inflammatory pathway as a novel therapeutic strategy for COVID-19. Front Immunol 2020;11:595342.

33. Cailotto C, Gomez-Pinilla PJ, Costes LM, et al. Neuroanatomical evidence indicating indirect modulation of macrophages by vagal efferents in the intestine but not in the spleen. PLoS One 2014;9:e87785.

34. Kalff JC, Schraut WH, Simmons RL, et al. Surgical manipulation of the gut elicits an intestinal muscularis inflammatory response resulting in postsurgical ileus. Ann Surg 1998;228:652–663.

35. Tsuchida Y, Hatao F, Fujisawa M, et al. Neuronal stimulation with 5-hydroxytryptamine 4 receptor induces anti-inflammatory actions via α7nACh receptors on muscularis macrophages associated with postoperative ileus. Gut 2011;60:638–647.

36. Reardon C, Duncan GS, Brüstle A, et al. Lymphocyte-derived ACh regulates local innate but not adaptive immunity. Proc Natl Acad Sci U S A 2013;110:1410–1415.

37. Pan J, Zhang L, Shao X, et al. Acetylcholine from tuft cells: the updated insights beyond its immune and chemosensory functions. Front Cell Dev Biol 2020;8:606.

38. Gautron L, Rutkowski JM, Burton MD, et al. Neuronal and nonneuronal cholinergic structures in the mouse gastrointestinal tract and spleen. J Comp Neurol 2013; 521:3741–3767.

39. Hollenhorst MI, Jurastow I, Nandigama R, et al. Tracheal brush cells release acetylcholine in response to bitter tastants for paracrine and autocrine signaling. FASEB J 2020;34:316–332.

40. Wolf-Johnston AS, Hanna-Mitchell AT, Buffington CA, et al. Alterations in the non-neuronal acetylcholine synthesis and release machinery in esophageal epithelium. Life Sci 2012;91:1065–1069.

41. Madisen L, Mao T, Koch H, et al. A toolbox of Cre-dependent optogenetic transgenic mice for light-induced activation and silencing. Nat Neurosci 2012;15:793–802.

42. Chassaing B, Aitken JD, Malleshappa M, et al. Dextran sulfate sodium (DSS)-induced colitis in mice. Curr Protoc Immunol 2014;104:15.25.1–15.25.14.

43. Bhave S, Arciero E, Baker C, et al. Enteric neuronal cell therapy reverses architectural changes in a novel diphtheria toxin-mediated model of colonic aganglionosis. Sci Rep 2019;9:18756.

44. Rahman AA, Robinson AM, Jovanovska V, et al. Alterations in the distal colon innervation in Winnie mouse model of spontaneous chronic colitis. Cell Tissue Res 2015;362:497–512.

45. Stavely R, Hotta R, Picard N, et al. Schwann cells in the subcutaneous adipose tissue have neurogenic potential and can be used for regenerative therapies. Sci Transl Med 2022;14:eabl8753.

46. Pan W, Rahman AA, Stavely R, et al. Schwann cells in the aganglionic colon of Hirschsprung disease can generate neurons for regenerative therapy. Stem Cells Transl Med 2022;11:1232–1244.

47. Weihe E, Tao-Cheng JH, Schäfer MK, et al. Visualization of the vesicular acetylcholine transporter in cholinergic nerve terminals and its targeting to a specific population of small synaptic vesicles. Proc Natl Acad Sci U S A 1996;93:3547–3552.

48. Qu ZD, Thacker M, Castelucci P, et al. Immunohistochemical analysis of neuron types in the mouse small intestine. Cell Tissue Res 2008;334:147–161.

49. Ting HA, von Moltke J. The immune function of tuft cells at gut mucosal surfaces and beyond. J Immunol 2019; 202:1321–1329.

50. Chassaing B, Srinivasan G, Delgado MA, et al. Fecal lipocalin 2, a sensitive and broadly dynamic non-invasive biomarker for intestinal inflammation. PLoS One 2012;7: e44328.

51. Koelink PJ, Wildenberg ME, Stitt LW, et al. Development of reliable, valid and responsive scoring systems for endoscopy and histology in animal models for inflammatory bowel disease. J Crohns Colitis 2018; 12:794–803.

52. Stavely R, Bhave S, Ho WLN, et al. Enteric mesenchymal cells support the growth of postnatal enteric neural stem cells. Stem Cells 2021;39:1236–1252.

53. Ott LC, Han CY, Mueller JL, et al. Bone marrow stem cells derived from nerves have neurogenic properties and potential utility for regenerative therapy. Int J Mol Sci 2023;24:5211.

54. Livak KJ, Schmittgen TD. Analysis of relative gene expression data using real-time quantitative PCR and the 2(-delta delta C(T)) method. Methods 2001;25:402–408.

Correspondence
Address correspondence to: Allan M. Goldstein, MD, Department of Pediatric Surgery, Massachusetts General Hospital, 55 Fruit Street, Warren 1151, Boston, Massachusetts 02114. e-mail: amgoldstein@mgb.org.